Supramolecular Structures of Low-Molecular-Weight Polybutadienes, as Studied by Dynamic Light Scattering, NMR and Infrared Spectroscopy

Jiří Podešva,* Jiří Dybal, Jiří Spěváček, Petr Štěpánek, and Peter Černoch

Institute of Macromolecular Chemistry, Academy of Sciences of the Czech Republic, Heyrovský Sq. 2, 162 06 Prague 6, Czech Republic

Received July 12, 2001

ABSTRACT: Three types of low-molecular-weight polybutadienes (bearing no or primary or secondary hydroxy groups on both chain ends), as well as their hydrogenated analogues, were studied by ^{1}H NMR and IR spectroscopies and by dynamic light scattering. In bulk and at room temperature, hydroxylated polymers form hydrophilic microdomains (knots) based on hydrogen bonds between two or more OH end groups; these knots gradually disintegrate with increasing temperature and above 100 °C, only OH/OH pairs can be present, as is seen from IR spectra. Fixation of more than two chain ends in a single knot leads to the spatial restriction of the segmental motion of the chain links which manifests itself by the broadening of ^{1}H NMR bands. With unsaturated, hydroxylated polymers, an intramolecular interaction between an OH end group and the adjacent C=C bond of the terminal monomer unit is possible which makes the formation of the intermolecular OH/OH bonding less probable. The dynamic light scattering method revealed the presence of large clusters in bulk; these supramolecular structures are bound together not only by hydrogen bonds but also by interactions between the aliphatic chains. With increasing temperature, intermolecular hydrophobic domains dissociate only for unsaturated polymers.

Introduction

For more than a decade, several laboratories including that of ours have been studying dynamic supramolecular structures (clusters) present in various polymeric materials, both in solution and in bulk. Thus, for example, clusters have been detected by dynamic (quasielastic) light scattering in semidilute solution of polystyrene,[1] concentrated solutions of polystyrene−polyisoprene diblock copolymer,[2] siloxane block copolymer melts,[3] or poly(ethylenepropylene)−poly(ethylethylene) diblock copolymer melts.[4] However, the physical nature of forces that give rise to the clusters remains a subject of hypotheses and probably depends on the material studied. Various authors have proposed different explanations, such as (i) formation of a physical network [poly(ethylene oxide) melts[5]], (ii) self-assembly of one of the polymeric components present in the mixture (diblock copolymers[6]), or (iii) long-range density fluctuations (polymers or glass-forming liquids[7]).

To extend the knowledge of these forces, we have decided to study supramolecular structures in such polymers which bear end groups able to form physical "knots" or domains, easily analyzed by, e.g., IR spectroscopy. As a model, we have chosen low-molecular-weight polybutadiene (liquid rubber, LR) with OH end groups on both ends. OH-telechelic LR is an interesting and technically useful material [among other applications, it is used as a macromolecular α,ω-diol for the production of polyurethanes (e.g., ref 8)].

Experimental Section

Materials. Three types of commercial low-molecular-weight, 1,2-rich polybutadienes, supplied by Kaučuk a.s., Kralupy n. Vlt., Czech Republic, under a common trademark Krasol, were used as model polymers and starting materials for hydrogenation. All of them were prepared by living anionic polymerization in polar media.[9] They are coded as LB (no OH end groups), LBH (secondary hydroxy groups on both chain ends introduced through the termination by propylene oxide), and LBHP (primary hydroxy groups on both chain ends through the termination by ethylene oxide). We tried to acquire Krasol batches with similar molecular weights and microstructures (see Table 1). All samples supplied were stabilized by Irganox 1520, its level (approximately 0.03 wt %) being by an order of magnitude lower than usual for standard applications.

Smaller portions of the stock Krasol samples were hydrogenated:[10] (i) in case of LBH, and LBHP, gaseous hydrogen and a Ziegler−Natta (nickel) catalyst was used to give the respective saturated analogues, HLBH and HLBHP; (ii) for LB, catalytic hydrogenation of which yielded insufficient degree of saturation, the diimide method (see, e.g., ref 10 and the references therein) was applied (still, however, not more than 92% saturation was attained), the product being coded as HLB. This difficulty in case of LB is in accordance with the previously reported, rather paradoxical finding[11] that the effectiveness of the nickel catalysts decreases with decreasing molecular weight of the polybutadiene substrate. The reason this is not true for LBH remains unclear. Molecular parameters of these hydrogenated analogues are also listed in Table 1.

Heptane (analytical grade, Lachema Brno, Brno, Czech Republic) for the measurements of IR spectra of dilute solutions of LBH, HLBH, LBHP, and HLBHP was used as received.

Methods. The IR spectra were measured on a Fourier transform infrared spectrometer Bruker IFS-55. Spectra were recorded at 2 cm^{-1} resolution. For treating the spectra, a commercial software OPUS (supplied by Bruker) was applied. The spectra of the heptane solutions were measured in the KBr cells having the thickness of 0.98 and 0.602 mm. For the measurements of the bulk, solvent-free samples, thin layers between the KBr windows were used. For the measurements of the infrared spectra at temperatures up to 160 °C, a homemade heated cell was used. The temperature was electronically controlled with ±1 °C accuracy. Before each measurement, the sample was equilibrated at the particular temperature for 5 min. A whole temperature cycle with a 10 °C step was always performed, starting at 25 °C; at a given

* Corresponding author. E-mail podesva@imc.cas.cz.

10.1021/ma011220f CCC: $20.00
Published on Web 11/27/2001

Table 1. Molecular Parameters of the Model Polymers Studied[a]

sample code	$10^{-3}M_n$[b]	M_w/M_n[b]	microstructure (%)[b]			functionality (%)[d]			h (%)[d]
			1,4-cis	1,4-trans	1,2	f_0	f_1	f_2	
LB	2.30	1.14	19.4	19.4	61.2	100	0	0	0
HLB	*c*	*c*	*e*	*e*	*e*	100	0	0	92[f]
LBH	2.37	1.13	19.6	18.0	62.4	0.1	1.1	98.8	0
HLBH	*c*	*c*	*e*	*e*	*e*	*c*	*c*	*c*	98.4[g]
LBHP	2.98	1.12	19.2	17.6	63.2	2.8	6.7	90.5	0
HLBHP	2.77	1.14	*e*	*e*	*e*	1.4	6.1	92.5	98.5[g]

[a] M_n and M_w are number- and weight-average molecular weights; f_0, f_1 and f_2 are fractions of polybutadiene chains with zero, one and two hydroxy end groups; h is the degree of hydrogenation of the olefinic double bonds. For coding the samples see the text. [b] Values supplied by the manufacturer. [c] Not determined. [d] Determined by ^{1}H NMR. [e] It is assumed that, after hydrogenation, the fraction of the 1-butene units is equal to that of 1,2-butadiene units of the precursor. [f] Samples hydrogenated by the diimide method. [g] Samples hydrogenated by the catalytic method.

temperature, the spectra were identical for both increasing and decreasing part of the cycle which means that the processes were reversible.

Molecular geometry optimizations and frequency calculations of the model methanol structures were performed with a Gaussian 98 program package[12] using the density functional theory (DFT) with the B3LYP functional[13] and Møller−Plesset second-order perturbation[14] (MP2) approaches. Geometries of the hydrogen-bonded configurations were completely optimized at the B3LYP/6-311+G(d,p) and MP2/6-31G(d) levels of theory.

High-resolution ^{1}H NMR spectra of the samples in bulk were measured in sealed 5 mm NMR tubes without deuterium lock with a Bruker Avance DPX 300 spectrometer operating at 300.1 MHz. Measurement conditions were as follows: 90° pulse width, 15.4 μs; relaxation delay, 4 s; spectral width, 5995 Hz; acquisition time, 1.37 s; eight scans. The temperature was maintained constant within ±0.2 K with a B-VT 2000 temperature unit.

The degree of hydrogenation was determined from analysis of 300.1 MHz ^{1}H NMR spectra of hydrogenated samples measured in $CDCl_3$ solutions. The following bands were used for quantitative analysis: resonance of methylene vinyl protons of 1,2 units of PB at 4.9 ppm (integrated intensity $I_{CH_2=}$), the region 5.3−5.8 ppm where are resonances of methine vinyl protons of 1,2 units and olefinic protons of 1,4 units of polybutadiene (integrated intensity $I_{CH=}$), resonance of methyl protons of hydrogenated 1,2 units at 0.8 ppm (integrated intensity I_{CH_3}), and the region 0.9−1.6 ppm where are resonances of other protons of hydrogenated polybutadiene, as well as resonance of methylene main chain protons of 1,2 units of polybutadiene (integrated intensity I_{CH+CH_2}). From the integrated intensities mentioned above the following quantities were determined: $A = (I_{CH_2=}/2)$; $B = I_{CH_3}/3$; $C = [I_{CH=} - (I_{CH_2=}/2)]$; $D = [I_{CH+CH_2} - I_{CH_2=} - (5I_{CH_3}/3)]/8$. The total degree of hydrogenation (in %) was determined as the expression $[B/(A + B + C + D) + D/(A + B + C + D)] \times 100$ where the first and second terms are the degrees of hydrogenation of original 1,2 units and 1,4 units, respectively. The microstructure (content of 1,4-cis, 1,4-trans and 1,2 units in unsaturated samples) was determined by the analysis of the olefinic region (4.8−5.7 ppm), as described in an earlier paper.[15]

The dynamic light scattering (DLS) instrument employed an ALV5000/E correlator. The light source was a Hewlett-Packard 125A laser with $\lambda_0 = 632$ nm. Temperature was controlled (±0.1 °C) with a Lakeshore 330 temperature controller. The scattered light was fed into an ALV double detector via a multimode optical fiber. In this unit, the signal is split by a cube beam splitter into two photomultipliers and discriminators. The correlator was operated in the crosscorrelation mode, which ensures that all artifacts due to afterpulsing and other imperfections do not affect the correlation function in the early time regime. The measured intensity correlation functions $g^2(t)$ were analyzed using nonlinear inverse Laplace transformation to obtain the distributions of relaxation times $A(\tau)$ according to eq 1, where α is an instrumental parameter. The transformation program REPES[16] was used. This program differs from the widely used program CONTIN in that it fits directly the measured intensity correlation function $g^2(t)$.

$$g^2(t) - 1 = \alpha[\int A(\tau) \exp(-t/\tau)\, d(\tau)]^2 \qquad (1)$$

Values of dynamic viscosities of the bulk polymer samples were obtained by a homemade viscometer of the Höppler type enabling measurements to be performed at various angles of the path of the ball and up to high temperatures. Calibration was done using glycerol, glycerol/water mixtures, and dioctyl phthalate as standards.

Thermal Stability. Since both light scattering and IR studies included measurements at as high temperatures as 160 °C, it was necessary to test the thermal stability of polymers, i.e., to check if any structural changes occur under such conditions. Samples of all the six LR's were put in small glass vessels, attached to a high-vacuum line and heated at 10^{-5} Torr/160 °C for 2 h to simulate the conditions of measurements. No changes in ^{1}H NMR spectra in comparison with unheated samples were detected. Similarly, SEC (1 mL of THF/min, refractometric detection, PL-1000, 8 × 600 mm column) gave virtually identical molecular weight distributions for heated and unheated samples.

Sample Preparations. Bulk polymer samples for DLS measurements were first pressure-filtered through a jacketed sintered-glass filter (5−15 μm porosity) directly into a cylindrical glass ampule (9 mm i.d.) equipped with a narrower neck and a small magnetic stirring bar. To reduce the high viscosity of the melt, the filter was kept at 70−80 °C. (Before filtration, dust was removed from the ampule by acetone vapors.) The ampule was then attached to a high-vacuum line, evacuated to 10^{-5} Torr, heated gradually up to 160 °C under slow stirring to degas the material until the evolution of bubbles stopped, and sealed.

A similar degassing procedure was applied for the preparation of the samples for viscosity measurements, except for filtration, which was omitted.

Results and Discussion

IR Spectroscopy: Interactions of the OH Groups in Bulk. Temperature dependences of the IR spectra were measured without solvent in the range from 25 to 160 °C for the hydroxylated samples (LBH, HLBH, LBHP, and HLBHP, Figure 1, parts a−d).

Peaks around 3600 cm^{-1} are assigned to the stretching vibrations of the OH groups which are not included in classical hydrogen bonding between two or more OH groups. Below, it will be suggested, however, that these hydroxy groups may be engaged in intramolecular OH/C=C interactions. In addition to the peak at 3600 cm^{-1}, which can be seen in the whole temperature range and for all hydroxylated LR's under study, a very intensive and broad band is present (ca. 3340 cm^{-1}) at room temperature which corresponds to a large variety of H-bonded microdomains (knots) formed between three and more hydroxy groups, e.g.:

Table 2. Calculated Binding Energies and OH Stretching Frequencies of Methanol and Its Hydrogen-Bonded Associates

calculation method	ΔE_0[a]	frequency[b]
B3LYP/6-311+G(d,p)		
monomer		3845 (30)
dimer	−3.68	3839 (45), 3692 (413)
trimer	−13.47	3610 (795), 3602 (848), 3547 (11)
tetramer	−25.02	3484 (170), 3448 (1846), 3447 (1849), 3359 (0)
MP2/6-31G(d)		
monomer		3793 (23)
dimer	−6.38	3776 (38), 3678 (362)
trimer	−20.72	3567 (728), 3561 (759), 3480 (8)
tetramer	−35.29	3476 (252), 3427 (1642), 3426 (1649), 3314 (0)

[a] Energies are given in kcal/mol; ΔE_0 is ZPVE-corrected binding energy calculated with respect to unassociated monomers. [b] Frequencies are given in cm^{-1} and IR intensities (km/mol) are enclosed in parentheses beside them.

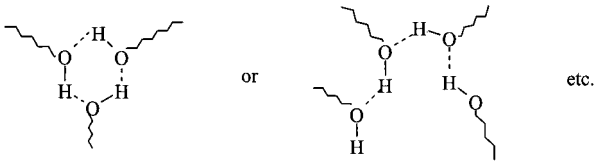

This broad band gradually diminishes with increasing temperature. Simultaneously, however, a peak at ca. 3530 cm^{-1}, which was overlapped by the broad band at room temperature, becomes visible. In accordance with model calculations performed for methanol (see below), this peak is assigned to H-bonded dimers of OH groups. We interpret the findings in Figure 1 so that, with increasing temperature, the mean number of OH groups per a single domain decreases until it reaches 2.

The results of the model calculations for methanol are presented in Table 2 from which it follows that wavenumbers of the OH stretching vibrations decrease from methanol monomer to methanol tetramer. Geometries of the hydrogen-bonded configurations are presented in Scheme 1.

The experimental results, as well as the model calculations, show that, upon heating, the "multihydroxy domains" present in bulk hydroxylated polymers disintegrate mostly into free OH groups (not H-bonded). Some of the domains are transformed into relatively stable linear sequences (several single hydroxylated chains arranged in a row) based on pairs of OH groups, schematically:

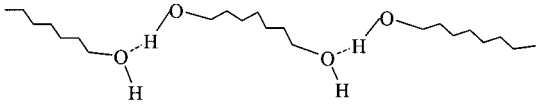

It follows from parts a and c of Figure 1 (LBH and LBHP) that, in unsaturated samples at room temperature, the band of the "nonbridged" hydroxy groups is split, being composed of two dominant overlapping parts at 3625 and 3594 cm^{-1}; with increasing temperature, intensities of both bands become equal.

We interpret this phenomenon as an intramolecular interaction between the OH end group and the adjacent olefinic C═C bond of the terminal monomer unit (OH/π interactions); similar interactions were found by IR spectroscopy[17,18] and also calculated from gas electron diffraction for 4-penten-1-ol (cf. ref 19) and 3-buten-2-ol (cf. ref 20). An additional support for the existence of the OH/C═C bonding which disappears upon hydrogenation was obtained by us from model calculations and IR spectra of the simplest low-molecular-weight models of the chain ends, that is, 5-hexen-2-ol and its saturated analogue, 2-hexanol. Contrary to 2-hexanol showing one relevant band at 3635 cm^{-1}, an additional band at 3598 cm^{-1} was found in IR spectra of 5-hexen-2-ol.

Scheme 1. Ab Initio Optimized Geometries of the Most Stable Structures of the Methanol Dimer, Trimer and Tetramer Calculated at the B3LYP/6-311+G(d,p) Level

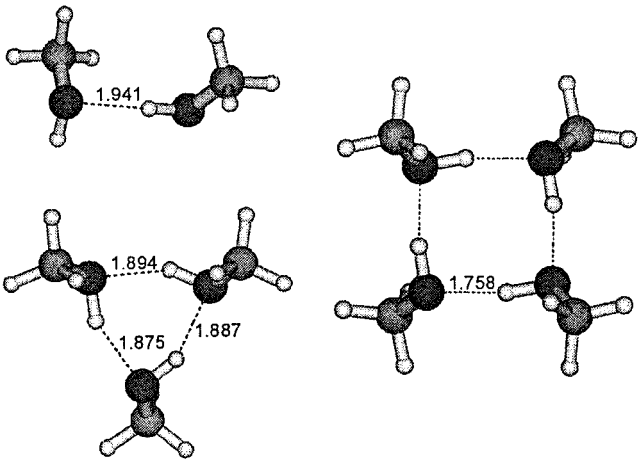

The distance between the two functional centers varies due to the rotation around three terminal single main-chain C−C bonds. It assumes its maximum value for fully extended chain-end and its minimum value for the coiled (pseudo-cyclic) one; naturally, the interaction between OH and C═C is possible only in the latter. We assume that the splitting reflects the existence of the two conformations: (i) coiled one (3594 cm^{-1}), when OH interacts with C═C; (ii) uncoiled one (3625 cm^{-1}), when OH is free and noninteracting. (Conversely, formation of classical hydrogen bonds between two or more OH groups is possible only if OH does not interact with C═C.) At higher temperature, the populations of the two structures are comparable.

In contrast, both hydrogenated analogues (HLBH and HLBHP, see Figure 1, parts b and d) exhibit a single, nonsplit band around 3630 cm^{-1} even at room temperature. Obviously, after hydrogenation of the olefinic double bonds, OH groups lose their C═C counterparts and the coiled conformations of the chain ends are no longer probable.

Since the terminal monomer unit of the unsaturated, hydroxylated LR's may have a 1,2 or 1,4-cis or 1,4-trans arrangement and the carbon atom bearing OH group is either asymmetrical (LBH, two different configurations) or symmetrical (LBHP), six different structures exist for LBH and three for LBHP. This is illustrated in Scheme 2 for the case of LBH.

IR Spectroscopy: Interactions of the OH Groups in Dilute Solution. The IR spectra of the dilute solutions (0.5 wt %) of the hydroxylated LR's in a nonpolar solvent (heptane) were recorded at room-temperature only. Upon further dilution, no changes of the spectra were observed. As follows from Figure 2a,b, the splitting of the bands of OH groups is observed again for the unsaturated samples only; it is due to the existence of coiled and uncoiled conformations of the chain ends and is much more pronounced than in bulk. (Small "shoulders" or inflections at 3614 cm^{-1} pertain to OH groups of the stabilizer.)

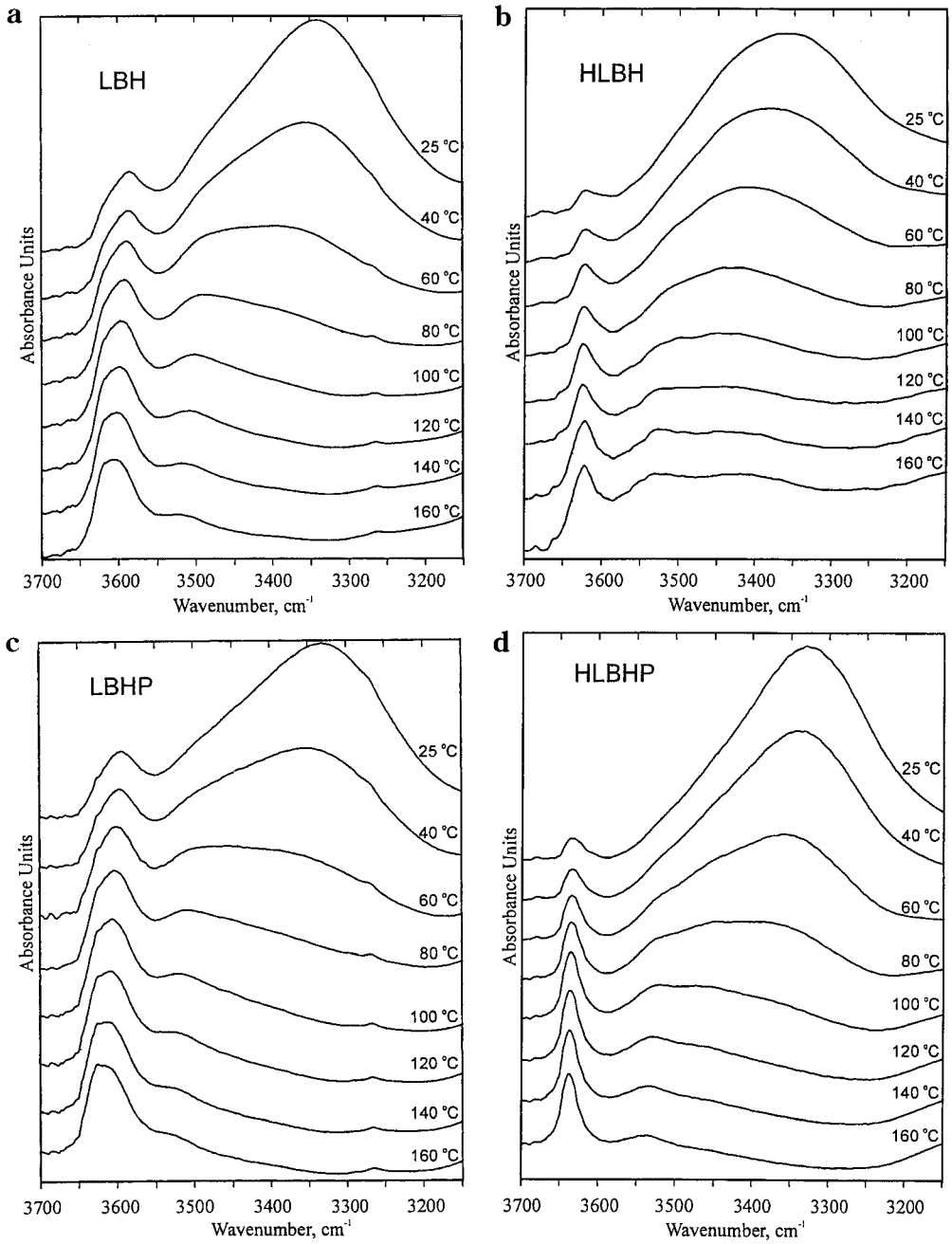

Figure 1. Parts of the FT IR spectra (parametrized by temperature) of polymers in bulk: (a) LBH; (b) HLBH; (c) LBHP; (d) HLBHP.

For LBH, the bands of OH groups were detected at 3633 and 3598 cm^{-1} (free OH groups and OH groups interacting with C═C, respectively); similarly, for LBHP, the corresponding wavenumbers are 3644 and 3605 cm^{-1}. Though no intermolecular OH/OH bonding is possible in dilute solutions, bands pertaining to hydrogen-bonded OH groups are still perceivable in the spectra in the range ~3500−3550 cm^{-1}, especially for the hydrogenated analogues; with HLBH, the peak is stronger than with HLBHP. Similarly as in bulk, the splitting of the OH bands disappears after the hydrogenation. It seems therefore that the chain ends of the dissolved unsaturated LR's may form coiled conformations based on OH/C═C bonding (similar to those of bulk polymers), whereas those of hydrogenated LR's tend to form intramolecular OH/OH bridges in dilute solution, resulting in the formation of macrocycles, in accordance with the fact that cyclization increases with increasing dilution:[21]

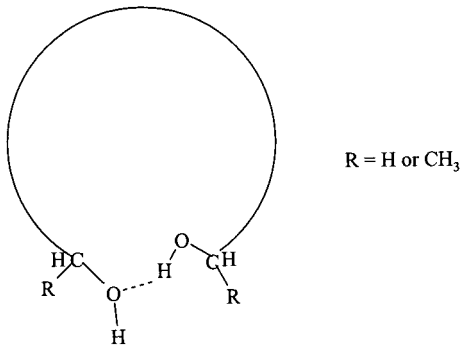

R = H or CH_3

Apparently, in dilute solutions, coiling of the chain ends due to the OH/C═C interaction hinders the forma-

Scheme 2. Conformation Equilibria between Coiled and Extended Chain-Ends of All Six Chain-End Configurations of LBH

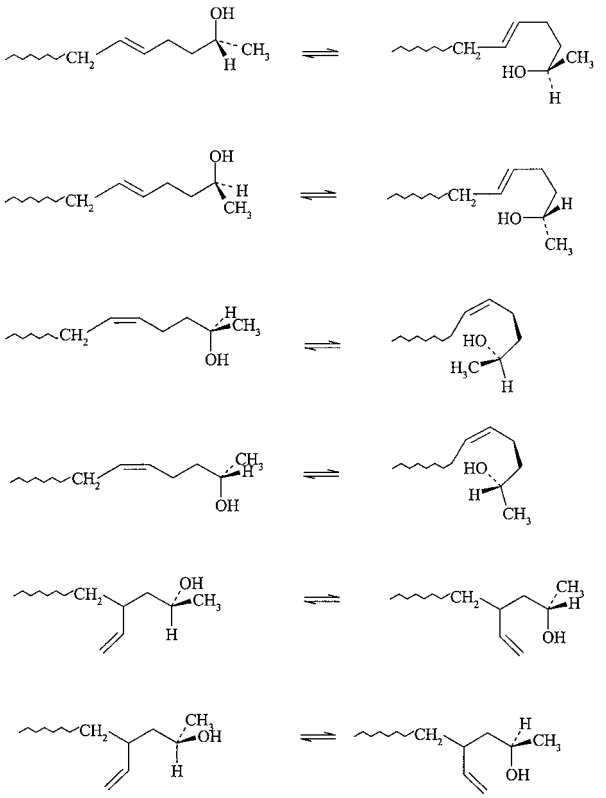

tion of the intramolecular OH/OH bridges. After hydrogenation, this hindrance disappears.

Chain Dimensions. To decide if a possible change of the chain flexibility upon hydrogenation may contribute to the formation of the rings discussed above, model calculations, based on the Porod−Kratky approximation,[22] were performed. The following simplifying assumptions were made:

(i) OH end groups, both primary and secondary, are disregarded (they have no influence on the overall dimensions of hydrogenated, as well as original chains).

(ii) In bulk, both unsaturated and hydrogenated chains exist in the Θ-state.

(iii) Reported characteristic ratios C_∞ are valid—4.9 and 5.8 (1,4-cis and 1,4-trans polybutadiene, respectively, see refs 23 and 24), 7.0 (1,2 polybutadiene, see[25]), and 8.0 and 4.5 [polyethylene and poly(1-butene), respectively, obtained by extrapolation from Figure 5 in ref 26].

Under these assumptions it was found that, rather surprisingly, the unperturbed root-mean-square end-to-end distance was 4.2 nm for both unsaturated and hydrogenated chains. This indicates that, for bulk LR's under study, hydrogenation virtually does not affect the unperturbed dimensions. After hydrogenation, the chain stiffness of pure 1,4-trans as well as 1,4-cis polybutadienes increases (polyethylene is formed), whereas that of pure 1,2 isomers decreases [poly(1-butene) is formed]. It seems therefore that the microstructure of the LR's under study is such that these effects just compensate each other.

Thus, of the two consequences of hydrogenation (i.e., the change of "microconformation" of the chain ends and the change of "macroconformation" of the whole chains),

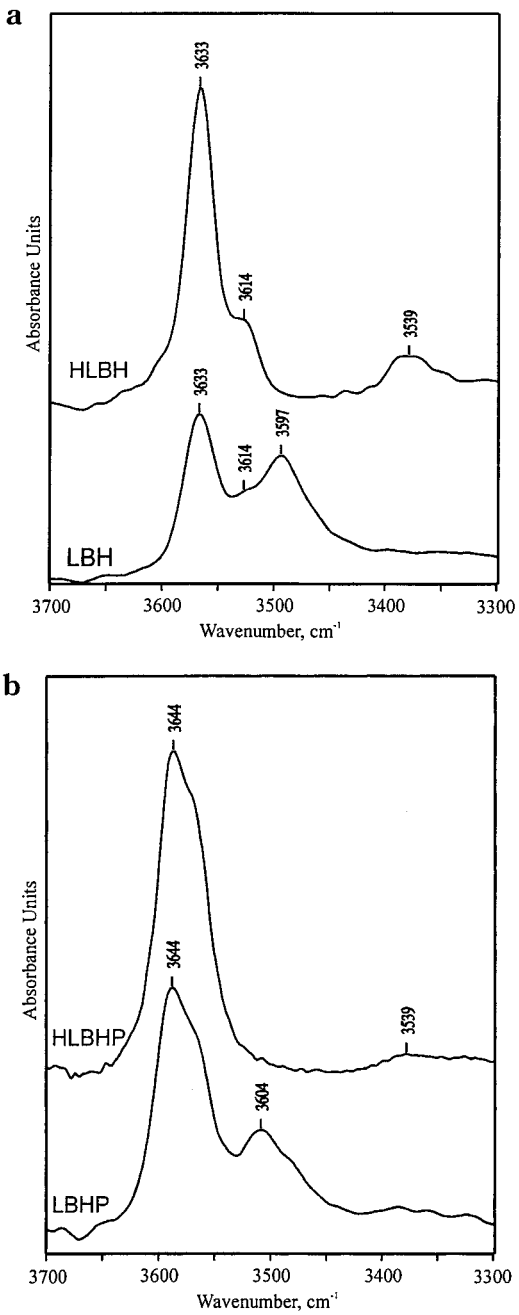

Figure 2. Parts of the FT IR spectra of polymers in dilute heptane solution at room temperature: (a) LBH and HLBH; (b) LBHP and HLBHP.

only the former is important for the formation of the intramolecular H-bonds.

Segmental Motion in Bulk by NMR. The influence of hydrophilic domains present in bulk OH-telechelic polybutadienes on the chain segmental mobility can be followed by ^{1}H NMR spectroscopy. For these polymers, conventional high-resolution spectra can be detected even in bulk. Using the spectra of LB and HLB measured at 27 °C as examples, the assignments of the individual bands are given in Figure 3. For the quantitative evaluation of the line widths ($\Delta\nu$) (measured at half the maximum height), two types of bands were chosen: (i) the main chain is represented by the band of $-CH_2-$ protons of the 1,4 unit (LB, LBH, LBHP) and the combined band of $-CH_2-$ (dominant) and $-CH-$ protons (HLB, HLBH, HLBHP); (ii) the side chain is represented by the line of $CH_2=$ protons of the 1,2 unit

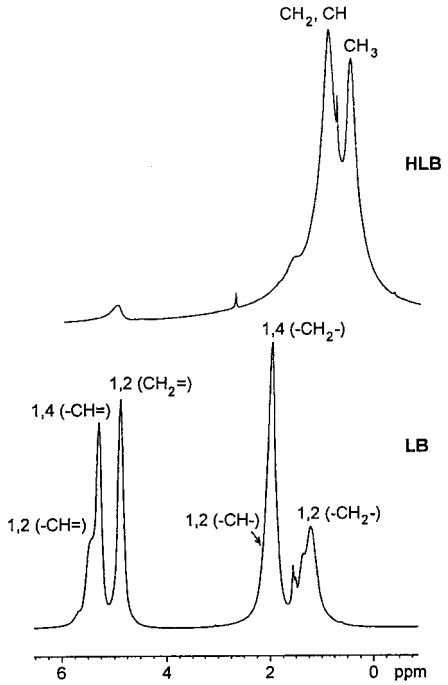

Figure 3. 300.1 MHz ^{1}H NMR spectra of LB and HLB in bulk at 27 °C.

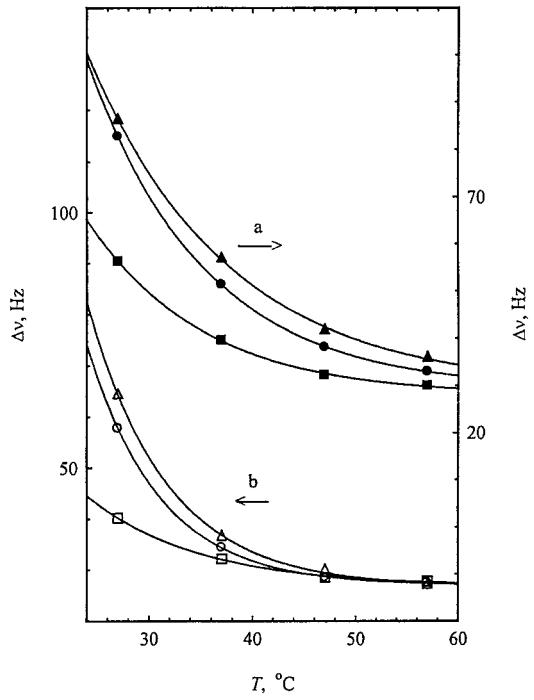

Figure 4. Temperature dependences of ^{1}H NMR line widths ($\Delta\nu$) of unsaturated polymers, as obtained from $-CH_2-$ bands of the 1,4 units (a, full data marks) and $CH_2=$ bands of the 1,2 units (b, empty data marks). Triangles, circles, and squares correspond to LBHP, LBH, and LB, respectively.

(LB, LBH, LBHP) and the line of CH_3- protons of the pendant ethyl group (HLB, HLBH, HLBHP).

A comparison of the line widths of all LR's under study is given in Figures 4a,b, 5a,b, and 6a,b. Generally, introducing the OH end groups on the chains causes broadening of all bands in the spectra at room temperature. This is a consequence of a spatial restriction of the segmental motion due to a fixation of chain ends in the hydrophilic microdomains. In other words, a physical network is formed, the knots of which (constituted by H-bonded OH groups) hinder the motion of its links.

NMR of Unsaturated Polymers. When OH end groups are introduced onto unsaturated chains (Figure 4a,b), the line width $\Delta\nu$ increases at room temperature by approximately 50 %, for the bands of both main and side chains. The increase is relatively small because only a fraction of these chain ends may enter the domains (knots). As described above for IR data, an equilibrium is established between the coiled and uncoiled conformations of a chain end, only the latter allowing the OH group to form intermolecular hydrogen bonds with other OH groups.

For non-hydroxylated chains, the decrease of the line width with increasing temperature is caused by releasing the segmental motion only. For hydroxylated chains, this releasing is combined with a decrease of the concentration of the knots and/or a decrease of an average number of OH groups per a single knot. A given knot of the physical network may hinder the segmental motion only if it contains three or more OH groups.

The fact that, at room temperature, the line widths in both parts a and b of Figure 4 are somewhat higher for the primary than for the secondary OH groups can be explained by a steric hindrance: if the methyls are absent, the knots are formed more easily and are stronger.

For the bands of the main chain (Figure 4a), the difference between the hydroxylated and non-hydroxylated polymer decreases with increasing temperature but remains perceptible even at 57 °C, whereas for the bands of the side chains (Figure 4b) the difference vanishes at the same temperature. This can be in connection with the existence of the side chain motion, in addition to the segmental rotation.

NMR of Hydrogenated Polymers. Introducing OH groups on the chain ends of the hydrogenated polymers causes more pronounced increase of the line widths (Figure 5a,b), especially for the polymers with primary OH groups where this increase amounts to ~125%, both for main-chain and side-chain bands. The reason is that the OH/C=C interactions disappear completely by hydrogenation, which makes all OH end groups free to form three- or multifunctional knots.

NMR: Pure Effect of the Knots. To separate the hindering effect of the knots alone (excluding all other effects), relative changes of the line widths caused by the introduction of OH end groups were plotted vs temperature in Figure 6a,b. This was expressed as $(\Delta\nu - \Delta\nu_0)/\Delta\nu_0$ where $\Delta\nu$ and $\Delta\nu_0$ are line widths of the hydroxylated and non-hydroxylated chains, respectively. It follows from these figures that the pure hindrance influence of the knots on the segmental motion decreases monotonically with increasing temperature (the concentration of the knots in the bulk and/or the mean number of the OH groups in a single knot decrease) and that this effect is much stronger for the primary hydroxy groups than for the secondary ones. While some of these dependences are almost linear (e.g., unsaturated polymers, main-chain bands), pronounced sigmoidal shape of the dependences observed, e.g., for main-chain bands of hydrogenated polymer indicates the significant reduction of the hindrance of the segmental motion in the range 35−50 °C.

Supramolecular Structures by DLS. The dynamic light scattering measurements performed with bulk polymers in the range 25−160 °C revealed that, as expected, diffusion modes of supramolecular structures

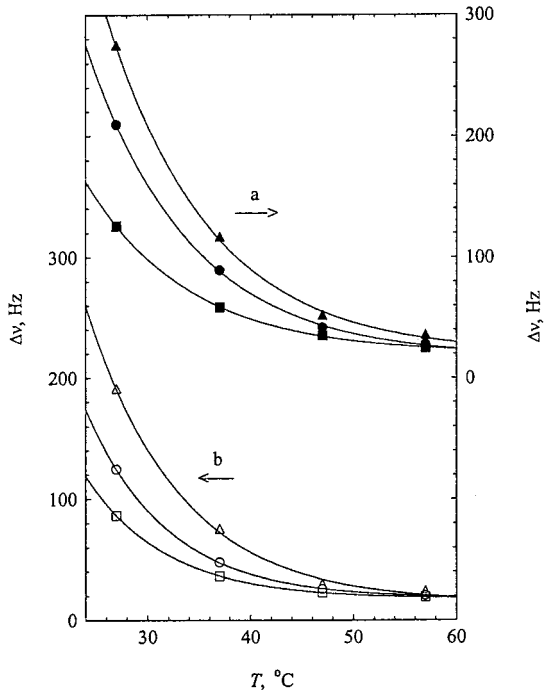

Figure 5. Temperature dependences of ^{1}H NMR line widths ($\Delta\nu$) of hydrogenated polymers, as obtained from $-CH_2-$, $-CH<$ bands (a, full data marks) and CH_3- bands (b, empty data marks). Triangles, circles, and squares correspond to HLBHP, HLBH, and HLB, respectively.

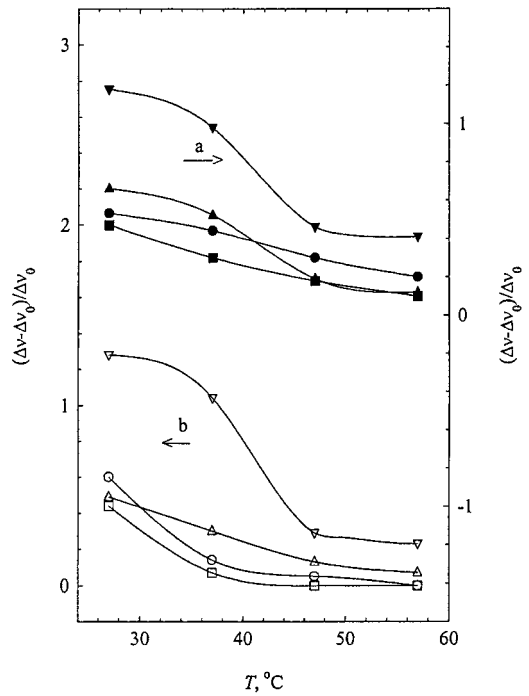

Figure 6. Temperature dependences of relative changes of ^{1}H NMR line widths caused by the introduction of OH end groups, as obtained from $-CH_2-$, $-CH<$ bands (a, full data marks) and $CH_2=$ and $-CH_3$ bands (b, empty data marks). $\Delta\nu$ and $\Delta\nu_0$ are line widths of the hydroxylated and non-hydroxylated chains, respectively; edge-up triangles, edge-down triangles, circles, and squares correspond to HLBH, HLBHP, LBHP, and LBH, respectively.

(clusters) are present in the relaxation time spectra for all 6 LR's under study. A typical 3D plot of scattered intensities vs relaxation time (τ, in μs) and temperature (T, in °C) is presented in Figure 7 with LBH as an example. The ridge running from log $\tau = 4.3$ at 150 °C to log $\tau = 7$ at 25 °C corresponds to the true clusters while the (disregarded) ridge running from log $\tau = 6.7$ at 150 °C to log $\tau = 8.5$ at 60 °C reflects the presence of very large particles, probably remaining dust.

To convert relaxation times into hydrodynamic radii, R_h, eq 2, derived from the Stokes−Einstein relation, was applied:

$$R_h = kT\tau q^2/6\pi\eta \qquad (2)$$

Here, k, T, q, and η are the Boltzmann constant, absolute temperature, absolute value of the scattering vector, and viscosity, respectively.

The temperature dependences of η, necessary for the conversion, were determined up to 160 °C. The experimental data were plotted in ln η vs T coordinates and fitted according to eq 3 (cf. ref 27):

$$\ln\eta = a + [b/(c + T)] \qquad (3)$$

A typical plot is presented in Figure 8 with LBH as an example, and the values of the parameters a, b, and c are listed in Table 3 for all six polymers.

The dependences of R_h on T are presented in Figure 9 from which it follows that, at room temperature, all polymers under study constitute clusters of similar dimensions (R_h ca. 150−200 nm). This similarity is in accordance with long accumulated but not yet explained experience:[3,28,29] when clusters are present in the material, their R_h usually ranges in the hundreds of nano-

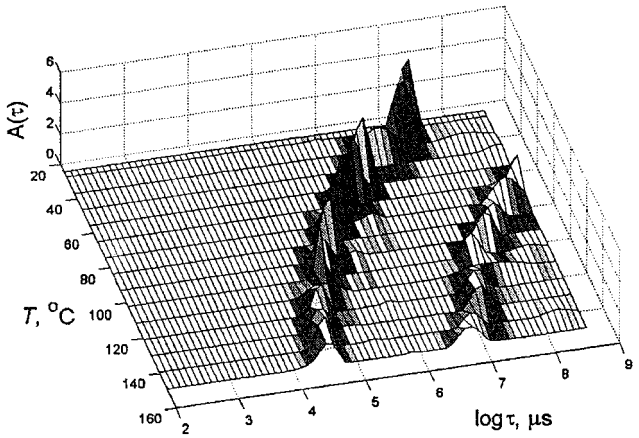

Figure 7. Three-dimensional image of the dependence of the scattered intensity $A(\tau)$ (arbitrary units) on temperature T (°C) and relaxation time τ (μs) for bulk LBH.

meters, irrespective of the molecular weight and chemical nature of the polymer, as well as the forces that bind macromolecules together. If 150 nm and 2300 g.mol^{-1} are used as the values of R_h at 25 °C and molecular weight of the LR, respectively, then, assuming that the density of the (spherical) cluster is not much different from 1.00 g·cm^{-3}, the mean number of macromolecules present in a single cluster is as large as about 4×10^6. However, it should be kept in mind that the R_h values are based on a model of diffusing objects (for which eq 2 is valid) and reflect instead dimensions of the hydrodynamically equivalent spheres.

According to Figure 9, the temperature dependences of R_h differ for unsaturated and hydrogenated polymers. With T increasing from 25 up to 160 °C, R_h of the former

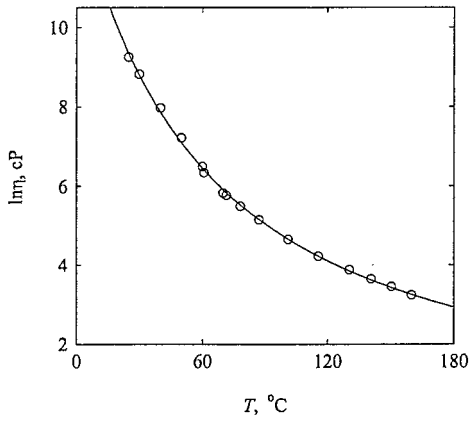

Figure 8. Typical viscosity (η, cP) vs temperature (T, °C) plot, as exemplified by bulk LBH.

Table 3. Values of Parameters *a*, *b*, and *c* Determined from the η vs T Plot (eq 3)

sample	*a*	*b*	*c*
LB	−0.984	1049	91.2
LBH	−0.608	851	60.6
LBHP	−0.537	1014	76.6
HLB	−1.69	1381	96.4
HLBH	−1.54	1229	82.5
HLBHP	−1.92	1433	92.5

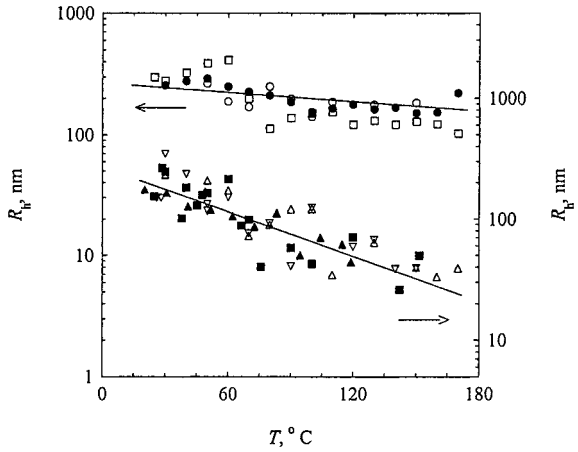

Figure 9. Results of dynamic light scattering: plot of cluster hydrodynamic radii (R_h, nm) vs temperature (T, °C). Upper set of data marks corresponds to hydrogenated polymers: HLB (●); HLBHP (□); HLBH (○). Lower set of data marks refers to unsaturated polymers: LBH (■); LB, first measurement (▲); LB, repeated measurement (△); LBHP (▽).

decreases by an order of magnitude, while that of the latter remains virtually constant.

We interpret these findings as follows. There are two parallel mechanisms of the formation and preservation of the clusters: In addition to the interaction of the chain ends (H-bonding discussed above, present only for hydroxylated LR's), also the inner parts of the chains may stick together by forces similar to those responsible for crystallization (this phenomenon is present for all six polymers). It is known that these forces are much stronger for aliphatic than for olefinic chains (e.g., refs 4 and 30). We assume that persistent hydrophobic domains may be formed by two or more macromolecules through an interaction of sequences of several ethylene units which undoubtedly exist in hydrogenated LR's.

In Scheme 3, the structure and possible thermal dissociation of the clusters of hydrogenated (A) and unsaturated (B) polymers is illustrated with hydroxylated LR's as examples. Upon heating, hydrophilic microdomains (OH knots) dissociate in both cases; in contrast, hydrophobic domains (pseudo-crystallic structures) dissociate only in case of unsaturated polymers while saturated polymers preserve their hydrophobic domains up to 160 °C. The processes are reversible: the same result is obtained even after several heating/cooling cycles. It should be kept in mind that the clusters are dynamic structures visible by DLS in a particular time window only: both OH knots and hydrophobic domains are continuously formed and destroyed.

Scheme 3. Hypothetical Representation of OH/OH and Aliphatic Knots in Bulk Hydroxylated Polymers and Their Dissociation upon Heating: Hydrogenated Polymer (above), Unsaturated Polymer (below)

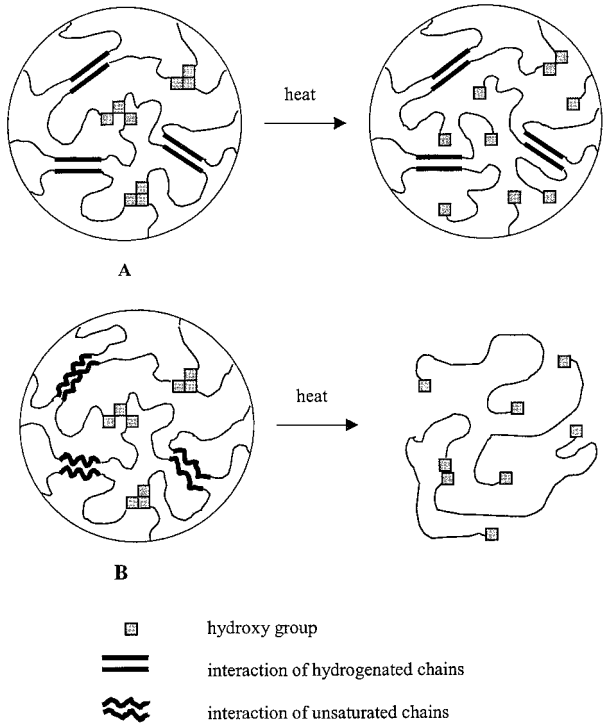

Conclusions

(i) In bulk and at room temperature, low-molar-mass polybutadienes, as well as their hydrogenated analogues, form (through pseudocrystalline interaction of parts of their chains) hydrophobic domains which contribute to existence of supramolecular clusters detectable by dynamic light scattering. These domains, and hence also the clusters, gradually and reversibly disintegrate with increasing temperature for original polybutadienes but persist in their hydrogenated derivatives.

(ii) When present, OH end groups contribute substantially to the formation and preservation of the clusters: hydrophilic microdomains based on hydrogen bonds between three and more OH groups exist in bulk OH-telechelic samples (be it unsaturated or hydrogenated analogues) at room temperature. These OH microdomains represent knots connected by hydrophobic links forming a physical network which hinders the segmental motion and manifests itself by broadening the bands of ^{1}H NMR spectra. With increasing temperature, however, the microdomains reversibly dissociate, as demonstrated by both NMR and IR spectroscopy. Above some 100−120 °C, only pairs of OH groups may persist in bulk.

(iii) It was proved by IR spectroscopy that, with unsaturated, hydroxylated samples, an interaction between an OH end group and the corresponding C═C bond of the adjacent terminal monomer unit takes place both in bulk and in dilute heptane solution due to the existence of coiled conformation of the chain ends. This intramolecular OH/C═C interaction makes the OH/OH hydrogen bonding less probable. After hydrogenation, OH end groups lose their C═C counterparts and the coiled conformations of the chain ends are no longer probable. In case of dilute heptane solutions, only intramolecular end-to-end OH/OH hydrogen bonding is possible, which leads to macrocycles.

Acknowledgment. This work was supported by the Grant Agency of the Academy of Sciences of the Czech Republic (Grant No. A4072902). The authors wish to thank to Dr. M. Bohdanecký for help with calculations of unperturbed chain dimensions. Much acknowledged is the material support from Kaučuk a.s., Kralupy n. Vlt., Czech Republic.

References and Notes

(1) Brown, W.; Štěpánek, P. *Macromolecules* **1988**, *21*, 1791.
(2) Balsara, N. P.; Štěpánek, P.; Lodge, T. P.; Tirrell, M. *Macromolecules* **1991**, *24*, 6227.
(3) Vogt, S.; Anastasiadis, S. H.; Fytas, G.; Fischer, E. W. *Macromolecules* **1994**, *27*, 4335.
(4) Štěpánek, P.; Lodge, T. P. *Macromolecules* **1996**, *29*, 1244.
(5) Walkenhorst, R.; Selser, J. C.; Piet, G. *J. Chem. Phys.* **1998**, *109*, 11043.
(6) Chitanvis, S. M. *Phys. Rev.* **1998**, *E 57*, 1921.
(7) Fischer, E. W. *Physica* **1993**, *A 201*, 183.
(8) Meyer, D. A. In *Rubber Technology*, 2nd ed.; Morton, M., Ed.; Van Nostrand Reinhold: New York, 1973; p 440.
(9) Pytela, J.; Sufčák, M.; Čermák, J.; Drobny, J. G. In *Polyurethanes Expo '98, Dallas, TX, Sept 17−20*; 1998, p 563.
(10) Podešva, J.; Holler, P. *J. Appl. Polym. Sci.* **1999**, *74*, 3203.
(11) Goodwin, D. E.; Willis, C. L. (Shell Oil Co.) US 5,1,66,277, 1992.
(12) Frisch, M. J.; Trucks, G. W.; Schlegel, H. B.; Scuseria, G. E.; Robb, M. A.; Cheeseman, J. R.; Zakrzewski, V. G.; Montgomery, J. A., Jr.; Stratmann, R. E.; Burant, J. C.; Dapprich, S.; Millam, J. M.; Daniels, A. D.; Kudin, K. N.; Strain, M. C.; Farkas, O.; Tomasi, J.; Barone, V.; Cossi, M.; Cammi, R.; Mennucci, B.; Pomelli, C.; Adamo, C.; Clifford, S.; Ochterski, J.; Petersson, G. A.; Ayala, P. Y.; Cui, Q.; Morokuma, K.; Malick, D. K.; Rabuck, A. D.; Raghavachari, K.; Foresman, J. B.; Cioslowski, J.; Ortiz, J. V.; Stefanov, B. B.; Liu, G.; Liashenko, A.; Piskorz, P.; Komaromi, I.; Gomperts, R.; Martin, R. L.; Fox, D. J.; Keith, T.; Al-Laham, M. A.; Peng, C. Y.; Nanayakkara, A.; Gonzalez, C.; Challacombe, M.; Gill, B.; Johnson, P. M. W.; Chen, W.; Wong, M. W.; Andres, J. L.; Gonzalez, C.; Head-Gordon, M.; Replogle, E. S.; Pople, J. A. *Gaussian 98, Revision A.7*; Gaussian, Inc.: Pittsburgh, PA, 1998.
(13) Becke, A. D. *J. Chem. Phys.* **1993**, *98*, 5648.
(14) Møller, C.; Plesset, M. S. *Phys. Rev.* **1934**, *46*, 618.
(15) Toman, L.; Vlček, P.; Sufčák, M.; Pleska, A.; Spěváček, J.; Holler, P. *Collect. Czech. Chem. Commun.* **2000**, *35*, 352.
(16) Jakeš, J. *Czech J. Phys.* **1988**, *B 38*, 1305.
(17) Schleyer, P. v. R.; Trifan, D. S.; Bacskai, R. *J. Am. Chem. Soc.* **1964**, *80*, 650.
(18) Sheppard, N. In *Hydrogen Bonding;* Hadzi, D., Thompson, H. W., Eds.; Pergamon Press: London, 1959; pp 85−105.
(19) Traetteberg, M.; Bakken, P.; Seip, R.; Lüttke, W.; Knieriem, B. *J. Mol. Struct.* **1985**, *128*, 191.
(20) Shishkov, I. F.; Shlykov, S.; Rousseau, B.; Peng, Z. H.; Van Alsenoy, C.; Geise, H. J.; Kataeva, O. N.; Herrebout, W. A.; Van der Veken, B. *J. Phys. Chem.* **2001**, *A 105*, 1039.
(21) Jacobson, H.; Stockmayer, W. H. *J. Chem. Phys.* **1950**, *18*, 1600.
(22) Flory, P. J. *Statistical Mechanics of Chain Molecules;* Interscience Publishers: John Wiley & Sons: New York, 1969; p 401.
(23) Mark, J. E. *J. Am. Chem. Soc.* **1966**, *88*, 4354.
(24) Mark, J. E. *J. Am. Chem. Soc.* **1967**, *89*, 6829.
(25) Zhongde, X.; Hadjichristidis, N.; Carella, J. M.; Fetters, L. J. *Macromolecules* **1983**, *16*, 925.
(26) Xu, Z.; Hadjichristidis, N.; Fetters, L. J.; Mays, J. W. *Adv. Polym. Sci.* **1995**, *120*, 1.
(27) Gutmann, F.; Simmons, L. M. *J. Appl. Phys.* **1952**, *23*, 977.
(28) Vogt, S.; Jian, T.; Anastasiadis, S. H.; Fytas, G.; Fischer, E. W. *Macromolecules* **1993**, *26*, 3357.
(29) Kanaya, T.; Patkowski, A.; Fischer, E. W.; Seils, J.; Glaser, H.; Kaji, K. *Acta Polym.* **1994**, *45*, 137.
(30) Štěpánek, P.; Lodge, T. P. In *Light Scattering, Principles and Development*; Brown, W., Ed.; Clarendon Press: Oxford, England, 1996; p 343.

MA011220F